I&EC research
Industrial & Engineering Chemistry Research

Article

pubs.acs.org/IECR

Modeling the Mini-Emulsion Copolymerization of *N*-Butyl Acrylate with a Water-Soluble Monomer: A Monte Carlo Approach

Shaghayegh Hamzehlou, Yuri Reyes,[†] and Jose R. Leiza*

POLYMAT, Kimika Aplikatua saila, Kimika Zientzien Fakultatea, University of the Basque Country UPV/EHU, Joxe Mari Korta Zentroa, Tolosa Hiribidea 72, 20018 Donostia-San Sebastián, Spain

Supporting Information

ABSTRACT: A Monte Carlo approach has been developed to simulate the miniemulsion polymerization of *n*-butyl acrylate with a water-soluble monomer, 2-hydroxyethyl methacrylate. The proposed simulation takes into account all the reactions in the aqueous and organic phases, as well as the entry of oligoradicals into the polymer particles by absorption and precipitation. The effect of the water-soluble monomer on the polymerization rate and on the molecular weight distribution of the polymer in the aqueous and organic phases has been studied. The addition of the water-soluble monomer retards the polymerization, though it had no significant effect on the molecular weight of the polymer produced in the particles; however, it increased the concentration of water-soluble polymer and its molecular weight. By this approach, it is possible to extract detailed information of polymer in the aqueous phase, such as the copolymer composition distribution.

INTRODUCTION

Emulsion polymerization is a very important technique to produce polymers in dispersed media, which are used in a myriad of relevant technological and industrial products, either as dry or dispersed polymers.[1,2] The mechanism of such multiphase systems is extremely complex not only due to the reactions taking place in different phases but also due to diffusional and monomer partitioning issues. The situation becomes even more complex when hydrophilic monomers are added in order to provide electrostatic stabilization[3−5] to tune the interactions between the polymer particles and a substrate (in the case of film forming latexes),[6] to place chemical groups capable of undergoing further reactions at the particle surface,[7] or to prepare hybrid polymers with functional monomers.[8] Although sophisticated models for emulsion polymerization are available,[9,10] in most cases, the reactions in the aqueous phase are neglected[11,12] despite the great influence of the water-soluble polymers formed during the reaction on the final properties of the product[1,5] or, if considered, the information of the hydrosoluble polymer formed in the aqueous phase is not provided, or the distribution of the acid groups is only accounted for.[13,14]

Another heterogeneous technique to produce dispersed polymers in water is miniemulsion polymerization.[15] The main mechanistic difference of miniemulsion polymerization, as compared to conventional emulsion polymerization, is that small droplets (in the nanometric range) are formed before the polymerization begins by applying a high shear to a coarse emulsion; if the nanodroplets are properly stabilized against coagulation and diffusional degradation (Ostwald ripening), these droplets become polymer particles. Ideally, no monomer transfer between droplets should take place in a well-formulated miniemulsion; namely, droplet nucleation is the key particle nucleation mechanism. Therefore, each monomer droplet may be treated as a completely segregated batch nanoreactor in terms of monomer content.[16] However, the partitioning of the monomer(s) between aqueous and organic phases is still relevant, as well as the reactions in water phase and the entry and exit of radicals.

Most of the models developed for emulsion and miniemulsion polymerization use a set of kinetic equations to compute the conversion of the monomer(s), along with partitioning and transport equations to calculate the concentration of the monomer in each phase, and use quite sophisticated numerical methods to compute the molecular weight distribution.[9,11,17,18] The situation becomes more complex when water-soluble monomers and complex kinetics are modeled. Acrylic monomers are representative of such complex kinetics because they undergo intra- and intermolecular chain transfer to the polymer that leads to the formation of midchain radicals (MCR); the intramolecular chain transfer decreases the average propagation rate coefficient and produces short branches and the intermolecular chain can produce long branches that, if terminated by combination, lead to high molecular weight and eventually gelled polymers.[19−21] Even in homogeneous polymerizations, the modeling of branches and gelled polymers by kinetic equations is rather challenging.

Stochastic approaches can be used to study complex kinetics and polymer microstructures, and they have been applied to study emulsion and miniemulsion polymerizations. Tobita pointed out that Monte Carlo (MC) simulation is suitable for emulsified systems because of the finite number of monomer molecules and polymer chains that form a single polymer particle and the fact that compartmentalization comes naturally in MC simulation.[22] A clear advantage of MC simulation is that the calculation of the molecular weight distribution is simple.

Special Issue: Massimo Morbidelli Festschrift

Received: September 25, 2013
Revised: December 9, 2013
Accepted: December 9, 2013
Published: December 9, 2013

dx.doi.org/10.1021/ie403182t | *Ind. Eng. Chem. Res.* 2014, 53, 8996−9003

Thus, kinetic Monte Carlo (KMC) simulation was used to analyze the miniemulsion polymerization of styrene initiated by an oil-soluble initiator. This simulation was useful to determine the mechanisms involved in particle nucleation in this system.[23] Controlled radical miniemulsion polymerization has been studied by Monte Carlo simulation in order to study the effect of particle diameter on polymerization rate and molecular weight distribution and the effect of RAFT agent on droplet nucleation.[24−27]

The purpose of this work is to present a kinetic Monte Carlo simulation approach of the miniemulsion copolymerization of an acrylic monomer (*n*-butyl acrylate, BA) and a water-soluble functional monomer (2-hydroxyethyl methacrylate, HEMA) as a representative system of a complex heterogeneous compartmentalized copolymerization in the presence of a water-soluble monomer. The simulation takes into account all the reactions in the water phase, the entry of the aqueous growing radicals by absorption and precipitation, the reactions within the polymer particles, and the exit of radicals. Moreover, by the KMC simulation, it is possible to obtain detailed information of microstructure of the copolymer, including the complete molecular weight distribution of the polymer present in the aqueous and organic phases.

SIMULATION DETAILS

The classic KMC algorithm proposed by Gillespie was implemented.[28,29] In the KMC algorithm, a control volume is defined. This volume is homogeneous and well-mixed. With this control volume and the Avogadro's constant, it is possible to calculate the number of molecules contained, provided that the concentrations of the components are defined. For each considered reaction, ν, a stochastic rate of reaction, R_ν, is defined as

$$R_\nu = C_\nu h_\nu \tag{1}$$

where C_ν is the stochastic rate coefficient (related with the experimental rate coefficients)[30] and h_ν is the number of possible combinations of the reactants involved in the νth reaction. Then, the probability of each reaction, P_ν, is

$$P_\nu = \frac{R_\nu}{\sum_{\nu=1}^{N} R_\nu} \tag{2}$$

where N is the total number of proposed reactions. A random number, $rand_1$, was used to select the reaction that takes place as follows:

$$\sum_{\nu=1}^{\mu-1} P_\nu < rand_1 < \sum_{\nu=1}^{\mu-1} P_\nu \tag{3}$$

with μ being the number of the selected reaction. The time step, τ, is calculated with another random number, $rand_2$

$$\tau = \frac{1}{\sum_{\nu=1}^{N} R_\nu} \ln \frac{1}{rand_2} \tag{4}$$

Once the reaction is chosen, the steps corresponding to the reaction are carried out. For example, initiator decomposition results in the elimination of an initiator molecule and the generation of two radicals; the propagation of a radical with a monomer increases the chain length of the radical by one unit while one monomer molecule is lost. This procedure allows obtaining detailed information of each polymer chain and deals with complex kinetics; additionally, it is a simple way to determine the complete molecular weight distribution.

In the present simulation approach the initial miniemulsion droplet volume defines the control volume; the solids content defines the control volume of the water phase. The most important assumption is that each droplet (and its own water volume) is considered as a batch reactor that does not exchange matter with the other droplets or particles but that does with its own water phase because of monomer partitioning and the entry and exit of radical species. This assumption seems to be reasonable if the miniemulsion droplets are well-stabilized by the surfactant and the hydrophobe. A monodisperse droplet size distribution is considered. The assumptions taken into account by the KMC simulation are the standard ones for the miniemulsion polymerization described by other kind of methodologies.[23,31−34]

It is worth noting that homogeneous nucleation (by growing and precipitation of oligoradicals in the aqueous phase) was not considered, although formation of hydrosoluble polymer and absorption of surface active and insoluble oligoradicals into the polymer particles was taken into account as discussed in the next section.

The concentration of each monomer in the aqueous and organic phases was calculated by using the partition coefficients, k_i^j

$$k_i^j = \frac{\varphi_i^j}{\varphi_i^w} \tag{5}$$

where φ_i^j is the volumetric fraction of component i in the phase j, and φ_i^w is the volumetric fraction of component i in the aqueous phase. These coefficients were considered constant through the reaction.[35] The values $k_{BA}^d = 714$[36] and $k_{HEMA}^d = 1.5$[37] were used as partition coefficients for *n*-BA and HEMA; these partitioning coefficients reflect the low water solubility of BA and the high hydrophilicity of HEMA.

REACTIONS IN THE AQUEOUS PHASE AND RADICAL ENTRY

Water-soluble initiators are the usual choice in (mini)emulsion polymerization. The radicals generated by the initiator (primary radicals) that are too soluble to be absorbed in the monomer droplets undergo some propagation steps in the aqueous phase. The resulting oligoradical is either water-soluble, surface active, or water insoluble, depending of the composition of the radical; additionally, these oligoradicals can terminate or undergo some transfer reaction in the water phase. In the homopolymerization of a sparingly water-soluble monomer (i.e., styrene or *n*-butyl acrylate), the addition of monomer units to a primary radical makes the oligoradical become surface active, so they can enter to the monomer droplet or polymer particle by absorption; if the oligoradical keeps growing and reaches the critical chain length, it becomes water insoluble and precipitates into the organic phase.[38,39] The situation is different in the case of a copolymerization with a water-soluble monomer because this monomer is at a higher concentration in the water phase, and its incorporation to the growing radical counteracts the effect of the sparingly water-soluble monomer. This is the situation of the *n*-BA/HEMA copolymerization, BA being a monomer with sparing water solubility and HEMA water-soluble. To take into account such relevant phenomena, the approach proposed by Zubitur et al. was used.[13] In this approach, the authors calculate

dx.doi.org/10.1021/ie403182t | Ind. Eng. Chem. Res. 2014, 53, 8996−9003

the aqueous molar solubility of all species in the aqueous phase, S_w, by

$$\log(S_w) = 0.8 - \log(k_{ow}) \quad (6)$$

where k_{ow} is the Rekker coefficient. The values of the group contributions to the Rekker coefficient are reported in Table 1

Table 1. Rekker Coefficients for Different Monomer and Contribution Groups[13,41]

Group contribution	k_{ow}
SO_4^-	−4.0
HEMA	−0.25
n-BA	2.54

for the initiator fragment, SO_4^-, and for *n*-BA and HEMA units. As in the present MC approach, where the composition of each radical generated in the aqueous phase is known in every moment, its S_w can be easily determined. If $S_w > 6.61 \times 10^{-4}$ mol/L, the oligoradical is totally water-soluble and can undergo any of the reactions except radical absorption. The maximum solubility is calculated considering a tristyryl sulfate radical as the shortest surface-active radical formed from initiator.[39] If $6.61 \times 10^{-4} > S_w > 1.0 \times 10^{-12}$ mol/L, the oligoradical becomes surface active and, additionally to chemical reactions in the water phase, it can also undergo absorption. Finally, if $S_w < 1.0 \times 10^{-12}$ mol/L it is considered that the radical undergoes instantaneous precipitation; this limit comes from relatively short oligomers that are insoluble (five styrene units). In Figure 1, the three regions as a function of copolymer composition are

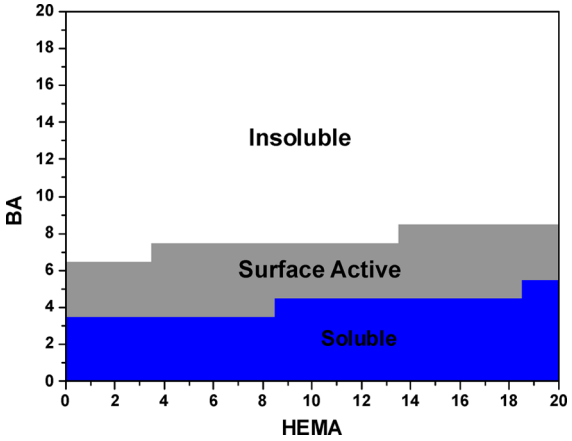

Figure 1. Solubility matrix of oligoradicals made of *n*-BA/HEMA in water phase with a terminal SO_4^- group.

depicted for the *n*-BA/HEMA system. The larger the *n*-BA content in the oligoradical, the more easily it becomes surface active or precipitates; on the other hand, the larger the HEMA content, the more hydrophilic the oligoradical is and it may remain in the aqueous phase. Daswani et al. recently also proposed a similar method for calculating of the solubility based on the hydrophilic lipophilic balance (HLB) of surfactants, but the calculation of solubility was not made in a quantitative basis.[40]

KINETIC SCHEME

The kinetic scheme of the *n*-BA/HEMA copolymerization is the one reported in a previous work[30] that includes: homo- and cross-propagation, chain transfer to monomer(s), intramolecular chain transfer of the acrylic component to the polymer, intermolecular chain transfer to the polymer and termination; the propagation and termination of the midchain radicals of the acrylic component and β-scission are also taken into account (see Supporting Information for a detailed description). The gel effect is also considered in the model as reported by Plesiss et al. for the emulsion polymerization of *n*-BA:[19]

$$k_t = k_{t0}\exp(-2.23\Phi_{polymer}) \quad (7)$$

where k_{t0} is the termination rate coefficient at zero conversion and $\Phi_{polymer}$ is the volume fraction of polymer in the polymer particles.

In addition to the chemical reactions, two first-order processes were considered to simulate the radical entry (as described above) and radical exit (further details in Supporting Information). As reported in the literature, radicals produced by a chain transfer to monomer are the only ones that can exit the polymer particles;[42] if the radical leaves the polymer particle, it can undergo any of the reactions in the aqueous phase accordingly. The kinetic scheme and the constants used in further simulations are the same as the ones we used in our previous work[30](see Supporting Information).

KMC IMPLEMENTATION AND MODEL OUTPUTS

As described above, once the droplet size and the solids content are given, the control volume of each phase is defined (monomer droplet and aqueous phase). One monomer droplet with its own water volume is simulated in a single run. The initiator concentration and comonomer ratio must also be given. All of the chemical reactions in the aqueous and organic phase, including entry and exit of radicals, are considered in the same ensemble to calculate their respective probability according to eq 2. To keep the randomness of the chemical system, once the reaction has been chosen by eq 3, the radical that must undergo such reaction is also chosen at random. Then, the reaction step is carried out and the information is saved (i.e., chain length and composition, number of MCR, etc.). In order to get results with statistical meaning, 500 particles were analyzed; this number is a good compromise between reliable results and computation time. Overall polymerization rate also can be calculated directly by MC by using the number of particles (N_p) as an input in the model.

Because by KMC the polymer chains are grown one by one, detailed information can be extracted from the simulation, in addition to what can be provided by solving the set of kinetic of equations that describe the evolution of the system (i.e., using a deterministic approach). For example, density of MCR (or degree of branching), concentration of long and short chain branches, the complete molecular weight distribution (including the oligomers that remain in the aqueous phase), the average composition of the polymers and chain length dependency of branching, composition, and so forth. It is worth mentioning that if polymer networks are formed, the entire molar mass distribution (soluble and gel fraction) is inherently obtained without any simplification or approximation that is required when deterministic models are used.[9,43,44] In order to demonstrate the capability of the model, in the following section, a series of miniemulsion copolymerizations of *n*-BA/HEMA with different experimental conditions are studied in detail.

dx.doi.org/10.1021/ie403182t | Ind. Eng. Chem. Res. 2014, 53, 8996−9003

RESULTS AND DISCUSSION

To show the applicability of the present simulation, the miniemulsion polymerization of *n*-BA at 70 °C in the presence of different amounts of HEMA (0, 0.5, 1.0, and 2.0 wt % with respect to *n*-BA) was studied in detail, at 24 wt % of solids content (SC) using 2 wt % of initiator (KPS) and assuming monomer droplets of 170 nm diameter. These systems are relevant from the synthetic and application points of view in order to produce waterborne adhesives for high-temperature applications.[45,46] Additionally, the system with 0.5 wt % of HEMA was studied at a higher solids content, 40 wt %.

Let us start our study by analyzing the kinetics of the miniemulsion polymerization and the influence of the HEMA content. Figure 2a shows that the miniemulsion polymerization

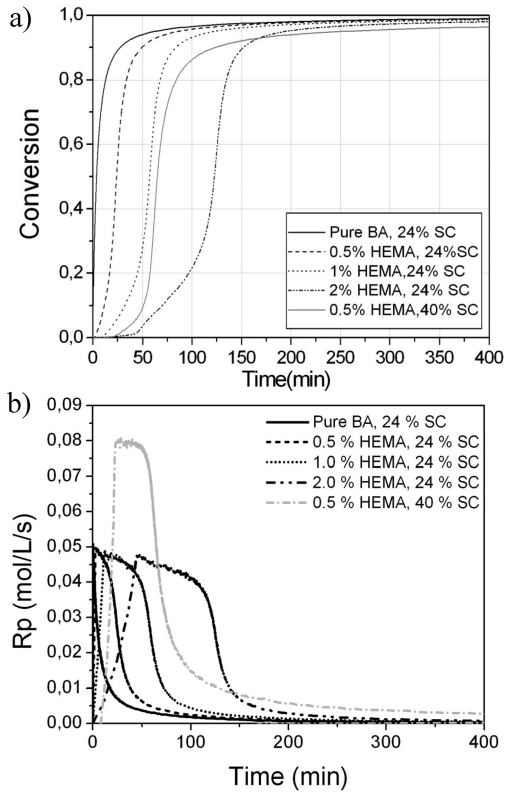

Figure 2. (a) Conversion and (b) polymerization rate versus time of the miniemulsion polymerization of pure *n*-BA and of *n*-BA with 0.5, 1, and 2 wt % of HEMA at 24 wt % SC; a higher solids content (40 wt %) for one system is also shown.

of pure *n*-BA at 24 wt % SC reached nearly 90% of conversion in around 25 min, which is in agreement with experimental findings.[47] Interestingly, the addition of the hydrophilic monomer retards the polymerization, but the polymerization rate is similar in all cases once the "retardation"-like period finishes, as displayed in Figure 2b.

This retardation is related to the reactions in the water phase that took place due to the larger presence of HEMA in this phase. As the amount of HEMA increased, the oligoradicals generated in the aqueous phase were richer in HEMA, which prevented its entry to the polymer particle because, as shown in Figure 1, the higher the HEMA content, the more soluble were the oligoradicals. Figure 2 clearly shows the importance of considering the reactions in the aqueous phase when a water-soluble monomer/polymer is used.[48]

On the other hand, by increasing the solids content at 0.5 wt % HEMA from 24 wt % to 40 wt %, it is possible to observe an enhanced retardation-like period and a higher polymerization rate. A higher solids content for the same monomer droplet size implies that less water was present and, therefore, the concentration of reactants in the aqueous phase was higher (including the initiator concentration), and so were the reaction rates. Enhanced retardation time can be then explained by a higher concentration of HEMA in the aqueous phase that decreased the entry of oligoradicals to the polymer particles and that increased of the hydrosoluble polymer (See Figure 1 in Supporting Information).

The effect of HEMA on the kinetics of the copolymerization (conversion curves and reaction rates) can be further explained by the development of the average number of radicals per particle, $\bar{n}$, which is shown in Figure 3 as a function of

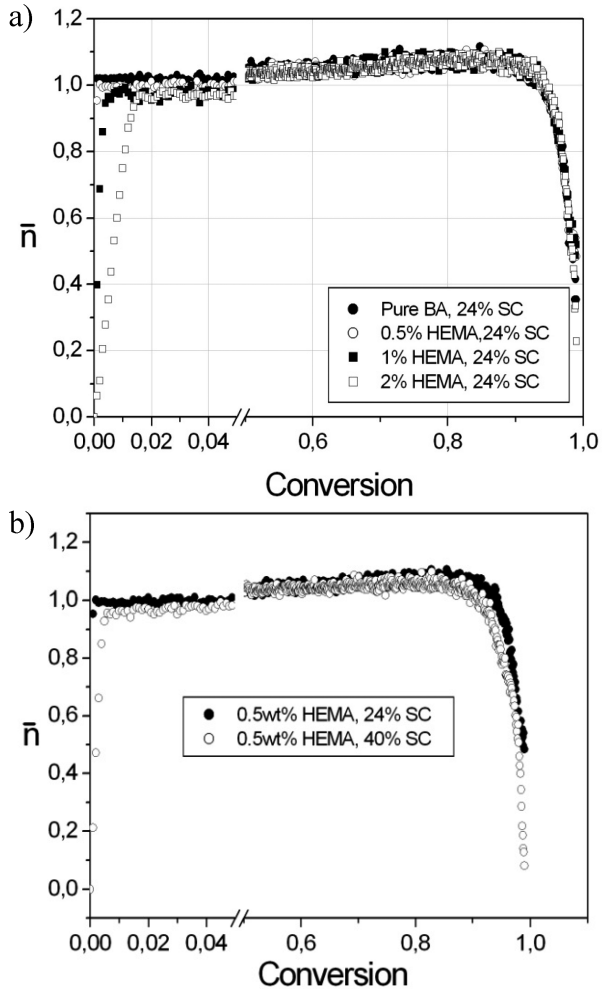

Figure 3. Average number of radicals per particle as a function of conversion. (a) effect of HEMA and (b) effect of solids content.

conversion. Figure 3 shows that $\bar{n}$ was above 1 during most of the polymerization. This is in agreement with literature reports that described the emulsion polymerization of *n*-BA as an example of Smith and Ewart case III kinetics, with $\bar{n} > 1$ (i.e., the rate of entry of radicals into particle is higher than termination rate).[12,31] Additionally, this monomer has low water solubility and the chain transfer to monomer is not relevant; therefore, the effect of radical exit is rather small.

dx.doi.org/10.1021/ie403182t | Ind. Eng. Chem. Res. 2014, 53, 8996−9003

Figure 3 shows a slight decrease in $\bar{n}$ as the HEMA content increases; but the main difference was the higher time (or conversion) required to reach to the plateau value of around one radical per particle.

It is interesting to compare the predictions of the simulation results presented in Figures 2 and 3 with experimental data available in the literature for a similar system. Chern et al. have investigated the effect of the addition of small amounts of hydrophilic monomers in the miniemulsion polymerization of styrene initiated by sodium persulfate, using as coestabilizers lauryl methacrylate (LMA) or stearyl methacrylate (SMA).[49,50] Interestingly, HEMA was one of the hydrophilic monomers analyzed. They found that the overall polymerization rate increased substantially by increasing the amount of HEMA in the formulation (HEMA 0, 0.3, 1, and 3 wt % based on the monomer). The macroscopic explanation was that the final number of particles increased (the particle size decreased) as the amount of HEMA increased in the formulation. This was attributed to a reduced percentage of droplet nucleation (in the range 20−38%) from the originally produced ones, and extensive homogeneous nucleation even in the polymerizations without HEMA. Comparison with this experimental data cannot be done in a straightforward manner because the simulation did not consider secondary nucleation. However, Chern et al. also calculated the polymerization rate per particle, which is directly comparable with the data obtained in the simulations. Both the simulation and the experimental results agreed in that the polymerization, rate per particle was slightly decreased by the increased amount of HEMA in the formulation. As can be seen in Figure 3, $\bar{n}$ slightly decreased as HEMA increased in the formulation.

Figure 3b also shows that increasing the solids content for the same HEMA concentration delayed $\bar{n}$ reaching the plateau value. This was due to the higher concentration of HEMA in the aqueous phase and the delayed entry of radicals into the polymer particles.

Figure 4 shows the effect of HEMA on the evolution of hydrosoluble polymer concentration. It can be seen that by increasing HEMA weight percentage, the polymer concentration in the aqueous phase sharply increased from the very beginning of the reaction, which explains again the decrease of $\bar{n}$ and the retardation period in the case of addition of HEMA. Note that if the secondary nucleation mechanism would have been included in the simulation, this would have resulted in a creation of a new crop of polymer particles.

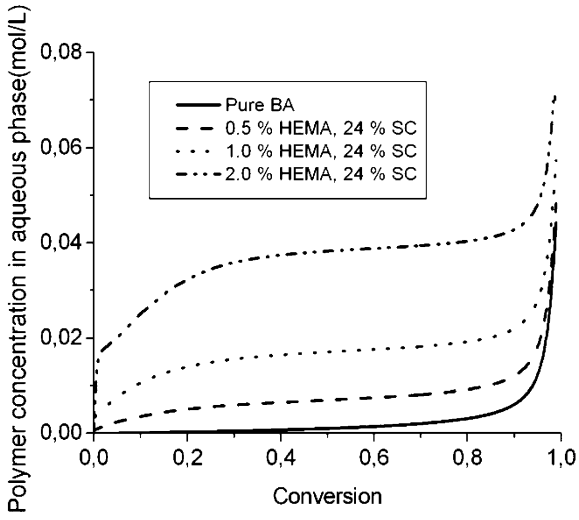

Figure 4. Evolution of polymer concentration in the aqueous phase for different content of HEMA in miniemulsion copolymerization of *n*-BA and HEMA.

One of the most difficult microstructure properties to obtain by conventional models is the complete molecular weight distribution, especially in compartmentalized and branched systems, for which MC simulation is especially suited. The predicted weight-average molecular weight obtained by KMC model (2.5×10^6 g/mol) is in good agreement with experimental data of the batch miniemulsion polymerization of pure *n*-BA carried out in a calorimetric reactor under the same conditions (SC = 24 wt %, KPS = 2 wt % with respect to the monomer), which reported a value of 2.84×10^6 g/mol.[47] Also noticeable is that the molecular weight distribution predicted by the KMC simulation did not predict the formation of gel polymer or a separated high molecular weight polymer ($>10^8$ g/mol), as it was experimentally measured and predicted by KMC model for the seeded semibatch emulsion polymerization of *n*-BA.[12] This has been attributed to the segregated nature of the miniemulsion polymerization, where each droplet behaves like a batch reactor and, hence, the polymer concentration in the polymer particles is lower than in a batch emulsion polymerization. The low concentration, together with the shorter reaction time, substantially reduces the intermolecular-chain transfer to polymer reaction and, hence, the formation of branched and cross-linked polymer.[32,51] Note that the maximum achievable molecular weight in a particle of 170 nm (assuming a density of 1 g/cm^3 and molar mass of 128 g/mol) is of the order of 10^9 g/mol, which is substantially higher than the size of the chains obtained in the miniemulsion polymerizations simulated shown in Figure 5.

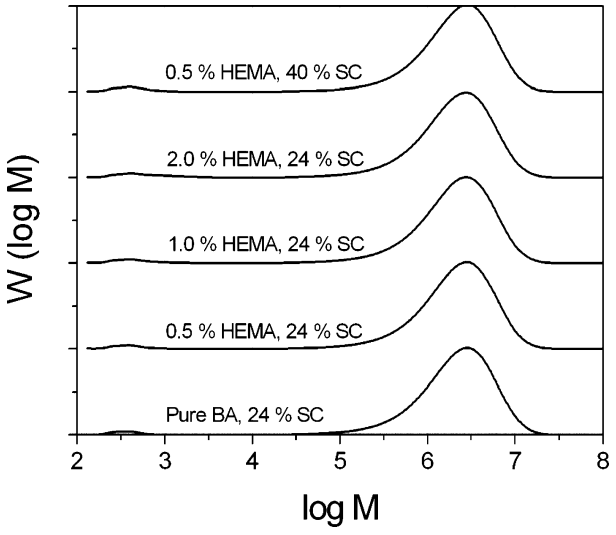

Figure 5. Simulated GPC molecular weight distribution of the copolymer *n*-BA/HEMA produced by batch miniemulsion copolymerization in the aqueous phase and in the polymer particles.

Although the molecular weights produced in the polymer particles did not change by increasing HEMA in the formulation (see Figure 5), its presence had a great effect on the amount of hydrosoluble polymer and the molecular weights of the polymer produced in the aqueous phase (see Figure 6 and also Figure 4, where the concentration of hydrosoluble

dx.doi.org/10.1021/ie403182t | Ind. Eng. Chem. Res. 2014, 53, 8996−9003

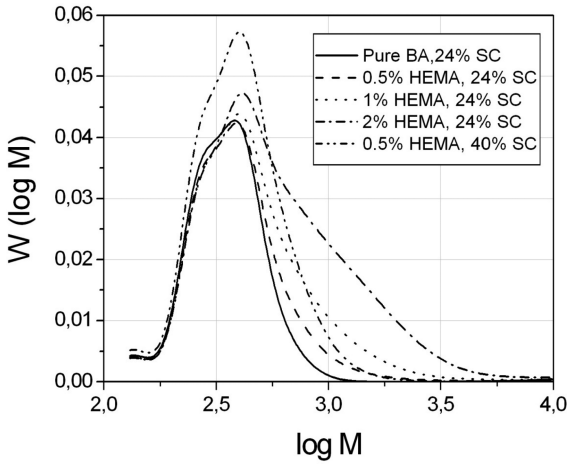

Figure 6. Simulated GPC molecular weight distribution of the copolymer *n*-BA/HEMA produced by batch miniemulsion copolymerization aqueous phase at full conversion.

chains was plotted). As can be seen in Figure 6, by increasing the HEMA content, the peak of the polymer that belonged to oligomers in the aqueous phase shifted to higher values and became broader. The amount of hydrosoluble polymer increases from 1.7 wt % to 3.1 wt % when increasing the content of HEMA from 0% to 2% in the formulation at 24 wt % solids. Note that some dead chains produced in the aqueous phase would violate the solubility matrix; in other words, longer chains than those allowed by the solubility matrix (depicted in Figure 1) produced by termination by combination in the aqueous phase are present in the MWD presented in Figure 5. Indeed, a fraction of these dead chains would have been the precursor of some new polymer particles if secondary nucleation would have been considered in the model. Moreover, by increasing the solids content, the amount of polymer formed in the water phase increased and the MWD became broader. The reason was that the radical concentration (because, as a result of the lower amount of water, initiator concentration was higher) and monomer concentration were higher in the aqueous phase at higher solids content, allowing more units of HEMA to be included in the polymer chains.

Figure 7 presents the copolymer composition distribution of the polymer that remains in the aqueous phase for the experiments simulated with 0.5 and 2 wt % of HEMA. The horizontal axis accounts for the number of HEMA units in the chain, whereas the vertical axis shows the *n*-BA units. The concentration of the oligoradicals is plotted in color scale, in mol/L. In the case of 0.5 wt % of HEMA, at low conversions, oligoradicals richer in HEMA were formed in the aqueous phase; the chains may contain up to 6 HEMA units in their composition. Nevertheless, the oligoradicals with 2 HEMA and 2 *n*-BA were the most abundant, at 10% conversion. By increasing conversion, oligomers richer in *n*-BA were formed, but the concentration of large chains containing HEMA was still relevant. At full conversion, the most abundant polymeric species in the aqueous phase were short oligoradicals containing 2 units of *n*-BA and none or only one unit of HEMA. This was mainly due to the depletion of HEMA from the aqueous phase. At HEMA contents of 2 wt % and low conversions, the copolymers had up to 10 units of HEMA in their composition. One can see the same trend in composition of oligoradicals by increasing conversion, but at full conversion,

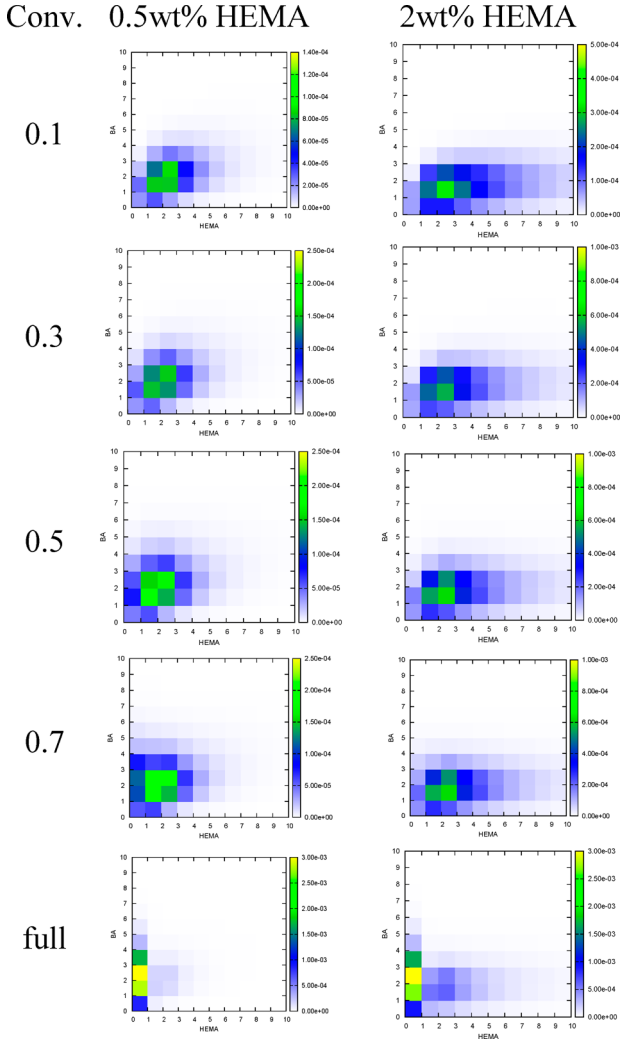

Figure 7. Copolymer composition distribution in aqueous phase for the systems with 0.5 and 2 wt % HEMA; the color scale is in mol/L.

although oligomers of *n*-BA were in larger quantity, the concentration of oligoradicals with up to 6 HEMA units in their composition was still relevant in this case. It should be noted that, the copolymer composition distributions of oligoradicals were plotted only up to 10 units of each monomer in their composition, although there were longer chains (richer in HEMA) created in the aqueous phase at very low concentration. Although these chains, in terms of concentration, have no contribution in the CCP graphs, they have a strong effect on the weight distribution (Figure 6) because of their higher molecular weight.

The advantage of the present simulation approach is that a complete characterization of the polymer in the aqueous phase can be obtained, in terms of molecular weight distribution, composition, and even composition as a function of chain length. These observations now can be compared with experimental results from MALDI-TOF MS[48] of the oligomers remaining in the aqueous phase, that is, using a technique with enough accuracy to provide the molecular weight and composition of these species. A combination of experimental MALDI-TOF MS and the KMC modeling could be very useful to test the operative radical entry mechanisms in the (mini)emulsion polymerization, which has been elusive so far. Figure 8 shows as an example of the conversion evolution of

dx.doi.org/10.1021/ie403182t | Ind. Eng. Chem. Res. 2014, 53, 8996−9003

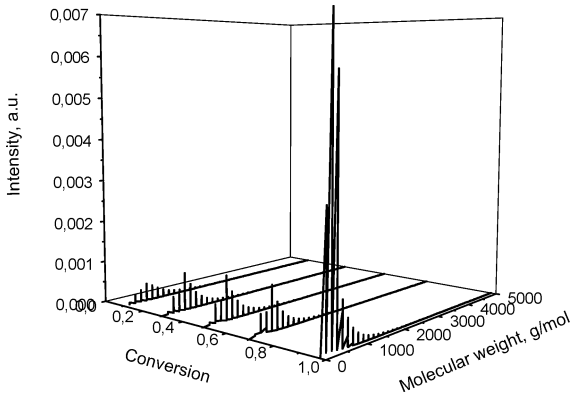

Figure 8. Evolution of the molecular weight distribution of the aqueous phase polymer for copolymerizations of *n*-BA with 2 wt % HEMA.

the molecular weight distribution of the polymer in the aqueous phase that can be directly compared to experimental MALDI-TOF MS spectra.

CONCLUSIONS

A Monte Carlo simulation approach to study the miniemulsion copolymerization of a monomer that has complex kinetics (*n*-BA) in the presence of a water-soluble monomer (HEMA) has been developed. The simulation takes into account all the reactions in the aqueous phase, considers the solubility, surface activity and water insolubility of the growing aqueous oligoradicals. The KMC provides microstructural properties given by other approaches, and additionally, KMC gives the complete molecular weight distributions of the polymer formed in the aqueous and organic phases, as well as the composition of the polymer. No simplifications are needed to account for the compartmentalization of the system and to determine the complete molecular weight distribution if branched or gelled polymers are formed. The model predicted very well the experimental finding that in the miniemulsion polymerization of *n*-BA gel is not formed. The characterization of the aqueous oligomers (molecular weight distribution and copolymer composition distribution) can be useful to determine the operative entry mechanisms by comparison with experimental results obtained by MALDI-TOF MS, for example.

With this simulation tool, the effect of HEMA content on the kinetics and polymer molecular weight and composition was studied. Ignoring the formation of new polymer particles by homogeneous nucleation, the presence of the water-soluble monomer retards the polymerization but does not substantially affect the polymerization rate, only slightly deceased due to a lower average number of radicals per particle. Furthermore the addition of HEMA did not modify the molecular weights produced in the polymer particle, but it did modify the polymer that remained in the water phase.

ASSOCIATED CONTENT

Supporting Information

Concentration of monomers and polymer in phases, flow diagram, kinetic scheme and rate coefficients. This information is available free of charge via the Internet at http://pubs.acs.org/.

AUTHOR INFORMATION

Corresponding Author

*J. R. Leiza. E-mail: jrleiza@ehu.es.

Present Address

†Departamento de Recursos de la Tierra, Universidad Autónoma Metropolitana Unidad Lerma (UAM-L). Av. Hidalgo Pte. 46, Col. La Estación, 52006, Lerma de Villada, México.

Notes

The authors declare no competing financial interest.

ACKNOWLEDGMENTS

The financial support of the Marie Curie Actions (initial training network, Nanopoly PITN-GA-2009-238700) and LIMPID project (FP7NMP-2012-2.2-6-310177) are gratefully acknowledged. J.R.L. and Y.R. acknowledge the funding by the University of the Basque Country UPV/EHU (UFI11/56), Basque Government (IT-303-07), and Ministry of Science and Innovation (CTQ2011-25572).

REFERENCES

(1) Urban, D.; Takamura, K. *Polymer Dispersions and their Industrial Applications*; Wiley-VCH: Weinheim, Germany, 2002.

(2) Asua, J. M. *Polymer Reaction Engineering*; Blackwell Publishing Ltd.: Oxford, U. K., 2007.

(3) Slawinski, M.; Meuldijk, J.; Van Herk, A. M.; German, A. L. Seeded Emulsion Polymerization of Styrene: Incorporation of Acrylic Acid in Latex Products. *J. Appl. Polym. Sci.* **2000**, *78*, 875−885.

(4) Shoaf, G. L.; Poehlein, G. W. Partition of Carboxylic Acids in an Emulsion Copolymerization System. *Ind. Eng. Chem. Res.* **1990**, *29*, 1701−1709.

(5) Zosel, A.; Heckmann, W.; Ley, G.; Mächtle, W. Chemical Heterogeneity in Emulsion Copolymers of Carboxylic Monomers. *Colloid Polym. Sci.* **1987**, *265*, 113−125.

(6) Gómez, R. M.; Reynoso, R.; Gómez, F.J. R.; Reyes-Mercado, Y. R.; Vázquez, F. Latex Film Performance of Styrene-acrylic Particles Functionalized with Acrylic Acid. *J. Appl. Polym. Sci.* **2009**, *113*, 553−557.

(7) Martínez, I. M.; Molina, A. M.; González, F. G.; Forcada, J. Synthesis of Amino-functionalized Latex Particles by a Multistep Method. *J. Polym. Sci., Part A: Polym. Chem.* **2001**, *39*, 2929−2936.

(8) Lopez, A.; Degrandi-Contraires, E.; Canetta, E.; Creton, C.; Keddie, J. L.; Asua, J. M. Waterborne Polyurethane-Acrylic Hybrid Nanoparticles by Miniemulsion Polymerization: Applications in Pressure-Sensetive Adhesives. *Langmuir* **2011**, *27*, 3878−3888.

(9) Butté, A.; Storti, G.; Morbidelli, M. Evaluation of the Chain Length Distribution in Free-Radical Polymerization, 2. Emulsion Polymerization. *Macromol. Theory Simul.* **2002**, *11*, 37−52.

(10) Broadhead, T. O.; Hamielec, A. E.; MacGregor, J. F. Dynamic Modelling of the Batch, Semi-batch and Continuous Production of Styrene/Butadiene Copolymers by Emulsion Polymerization. *Macromol. Chem. Phys.* **1985**, *10*, 105−128.

(11) Arzamendi, G.; Asua, J. M. Modeling Gelation and Sol Molecular Weight Distribution in Emulsion Polymerization. *Macromolecules* **1995**, *28*, 7479−7490.

(12) Arzamendi, G.; Leiza, J. R. Molecular Weight Distribution (Soluble and Insoluble Fraction) in Emulsion Polymerization of Acrylate Monomers by Monte Carlo Simulations. *Ind. Eng. Chem. Res.* **2008**, *47*, 5934−5947.

(13) Zubitur, M.; Armitage, P. D.; Amor, S. B.; Leiza, J. R.; Asua, J. M. Mathematical Modeling of Multimonomer (Vinylic, Divinylic, Acidic) Emulsion Copolymerization Systems. *Polym. React. Eng.* **2003**, *11*, 627−662.

(14) Calvo, I.; Hester, K.; Leiza, J. R.; Asua, J. M. Mathematical Modeling of Carboxylated SB Latexes. *Macromol. React. Eng.* **2013**, DOI: 10.1002/mren.201300168.

(15) Ugelstad, J.; El-Aasser, M. S.; Vanderhoff, J. W. Emulsion Polymerization: Initiation of Polymerization in Monomer Droplets. *J. Polym. Sci. Polym. Lett.* **1973**, *11*, 503−513.
(16) Asua, J. M. Miniemulsion Polymerization. *Prog. Polym. Sci.* **2002**, *27*, 1283−1346.
(17) Lichti, G.; Gilbert, R. G.; Napper, D. H. Molecular Weight Distribution in Emulsion Polymerizations. *J. Polym. Sci. Polym. Chem. Ed.* **1980**, *18*, 1297−1323.
(18) Storti, G.; Polotti, G.; Cociani, M.; Morbidelli, M. Molecular Weight Distribution in Emulsion Polymerization.I. The Homopolymer Case. *J. Polym. Sci. Polym. Chem.* **1992**, *30*, 731−750.
(19) Plessis, C.; Arzamendi, G.; Leiza, J. R.; Schoonbrood, H. A. S.; Charmot, D.; Asua, J. M. A Decrease in Effective Acrylate Propagation Rate Constants Caused by Intermolecular Chain Transfer. *Macromolecules* **2000**, *33*, 4−7.
(20) Plessis, C.; Arzamendi, G.; Leiza, J. R.; Schoonbrood, H.; Charmot, D.; Asua, J. M. Modeling of Seeded Semibatch Emulsion Polymerization of *n*-BA. *Ind. Eng. Chem. Res.* **2001**, *40*, 3883−3894.
(21) Yamada, B.; Azukizawa, M.; Yamazoe, H.; Hill, D. J. T.; Pomery, P. J. Free Radical Polymerization of Cyclohexyl Acrylate Involving Inter Conversion Between Propagating and Mid-chain Radicals. *Polymer* **2000**, *41*, 5611.
(22) Tobita, H.; Yamamoto, K. Network Formation in Emulsion Crosslinking Copolymerization. *Macromolecules* **1994**, *27*, 3389−3396.
(23) Rawlston, J. A.; Guo, J.; Schork, F. J.; Grover, M. A. A Kinetic Monte Carlo Study on the Nucleation Mechanisms of Oil-soluble Initiators in the Miniemulsion Polymerization of Styrene. *J. Polym. Sci., Part A: Polym. Chem.* **2008**, *46*, 6114−6128.
(24) Tobita, H. Threshold Particle Diameters in Miniemulsion Reversible-Deactivation Radical Polymerization. *Polymers* **2011**, *3*, 1944−1971.
(25) Luo, Y.; Yu, B. Monte Carlo Simulation of Droplet Nucleation in RAFT Free Radical Miniemulsion Polymerization. *Polym.-Plast. Technol. Eng.* **2004**, *43*, 1299−1321.
(26) Tobita, H. Fundamentals of RAFT Miniemulsion Polymerization Kinetics. *Macromol. Symp.* **2010**, *288*, 16−24.
(27) Tobita, H.; Yanase, F. Monte Carlo Simulation of Controlled/Living Radical Polymerization in Emulsified Systems. *Macromol. Theory Simul.* **2007**, *16*, 476−488.
(28) Gillespie, D. T. Exact Stochastic Simulation of Coupled Chemical Reactions. *J. Phys. Chem.* **1977**, *81*, 2340−2361.
(29) Gillespie, D. T. Stochastic Simulation of Chemical Kinetics. *Annu. Rev. Phys. Chem.* **2007**, *58*, 35−66.
(30) Hamzehlou, S.; Reyes, Y.; Leiza, J. R. Detailed Microstructure Investigation of Acrylate/Methacrylate Functional Copolymers by Kinetic Monte Carlo Simulation. *Macromol. React. Eng.* **2012**, *6*, 319−329.
(31) Costa, C.; Timmermann, S. A. S.; Pinto, J. C.; Araujo, P.h.h.; Sayer, C. Compartmentalization Effects on Miniemulsion Polymerization with Oil-Soluble Initiator. Macromol. *React. Eng.* **2013**, *7*, 221−231.
(32) González, I.; Paulis, M.; de la Cal, J. C.; Asua, J. M. Mini)emulsion Polymerization: Effect of the Segregation Degree on Polymer Architecture. *Macromol. React. Eng.* **2007**, *1*, 635−642.
(33) Rodriguez, V. S.; Asua, J. M.; El-Aasser, M. S.; Silebi, C. A. Mathematical Modeling of Seeded Miniemulsion copolymerization for Oil-soluble Initiator. *J. Polymer Sci., Part B: Polym. Phys.* **1991**, *29*, 483−500.
(34) Rodriguez, V. S.; El-Aasser, M. S.; Asua, J. M.; Silebi, C. A. Miniemulsion Copolymerization of Styrene-Methyl Methacrylate. *J. Polym. Sci., Part A: Polym. Chem.* **1989**, *27*, 3659−3671.
(35) Gugliotta, L. M.; Arzamendi, G.; Asua, J. M. Choice of Monomer Partition Model in Mathematical Modeling of Emulsion Copolymerization Systems. *J. Appl. Polym. Sci.* **1995**, *55*, 1017−1039.
(36) Vicente, M.; Leiza, J. R.; Asua, J. M. Simultaneous Control of Copolymer Composition and MWD in Emulsion Copolymerization. *AIChE J.* **2001**, *47*, 1594−1606.
(37) Tripathi, A. K.; Sundberg, D. C. Partitioning of Functional Monomers in Emulsion Polymerization: Distribution of Carboxylic Acid Monomers between Water and Multimonomer Systems. *Ind. Eng. Chem. Res.* **2013**, *52*, 9763−9769.
(38) Gilbert, R. G. *Emulsion polymerization, a mechanistic approach*, Academic Press Inc.: San Diego, CA, 1995.
(39) Maxwell, I. A.; Morrison, B. R.; Napper, D. H.; Gilbert, R. G. Entry of Free Radicals into Latex Particles in Emulsion Polymerization. *Macromolecules* **1991**, *24*, 1629−1640.
(40) Daswani P. Entry in Emulsion Copolymerization. Ph.D. Thesis, Eindhoven University of Technology, 2012.
(41) Mannhold, R.; Rekker, R. F. The Hydrophobic Fragmental Constant Approach for Calculating log P in Octanol/Water and Aliphatic Hydrocarbon/Water Systems. *Perspect. Drug Discovery Des.* **2000**, *18*, 1−18.
(42) Asua, J. M. A New Model for Radical Desorption in Emulsion Polymerization. *Macromolecules* **2003**, *36*, 6245−6251.
(43) Arzamendi, G.; Sayer, C.; Zoco, N.; Asua, J. M. Modeling of MWD in Emulsion Polymerization: Partial Distinction Approach. *Polym. React. Eng.* **1998**, *6*, 193.
(44) Teymour, F.; Campbell, J. D. Analysis of the Dynamics of Gelation in Polymerization Reactors Using the Numerical Fractionation Technique. *Macromolecules* **1994**, *27*, 2460−2469.
(45) Lopez, A.; Reyes, Y.; Degrandi-Contraires, E.; Canetta, E.; Creton, C.; Asua, J. M. Waterborne Hybrid Polymer Particles: Tuning of the Adhesive Performance Controlling the Hybrid Microstructure. *Eur. Polym. J.* **2013**, *49*, 1541−1552.
(46) Degrandi-Contraires, E.; Lopez, A.; Reyes, Y.; Asua, J. M.; Creton, C. Waterborne Polyurethane/Acrylic Soft Adhesives. *Macromol. Mat. Eng.* **2013**, *298*, 612−623.
(47) Yadav, A. K.; Barandiaran, M. J.; de la Cal, J. C. Effect of the Polymerization Technique and Reactor Type on the Poly(n-butyl acrylate) Microstructure. *Macromol. React. Eng.* **2013**, DOI: 10.1002/mren.201300159.
(48) Daswani, P.; Rheinhold, F.; Ottink, M.; Staal, B.; van Herk, A. Method to Isolate and Characterize Oligomers Present in the Aqueous Phase in Emulsion copolymerization. *Eur. Polym. J.* **2012**, *48*, 296−308.
(49) Chern, C.-S.; Sheu, J.-C. Effects of 2-Hydroxyalkyl Methacrylates on the Styrene Miniemulsion Polymerization Stabilized by SDS and Alkyl Methacrylates. *J. Polym. Sci., Part A: Polym. Chem.* **2000**, *38*, 3188−3199.
(50) Chern, C.-S.; Sheu, J.-C. Effects of Carboxylic Monomers on the Styrene Miniemulsion Polymerizations Stabilized by SDS/alkyl Methacrylates. *Polymer* **2001**, *42*, 2349−2357.
(51) Li, D.; Sudol, E. D.; El-Aasser, M. S. Miniemulsion and Conventional Emulsion Copolymerization of Styrene and Butadiene:Effect of Process on the Gel Content. *J. Appl. Polym. Sci.* **2006**, *102*, 4616−4622.